THE JOURNAL OF BIOLOGICAL CHEMISTRY
Vol. 277, No. 10, Issue of March 8, pp. 7838–7848, 2002
Printed in U.S.A.

Rapid and Selective Binding to the Synaptic SNARE Complex Suggests a Modulatory Role of Complexins in Neuroexocytosis*

Received for publication, October 2, 2001, and in revised form, December 17, 2001
Published, JBC Papers in Press, December 20, 2001, DOI 10.1074/jbc.M109507200

Stefan Pabst‡, Martin Margittai‡§, Darius Vainius¶, Ralf Langen‖, Reinhard Jahn‡, and Dirk Fasshauer‡**

From the Departments of ‡Neurobiology and ¶Molecular Biology, Max Planck Institute for Biophysical Chemistry, Göttingen D-37077, Germany and the ‖Institute for Genetic Medicine and Neurogenetic Institute, Department of Biochemistry and Molecular Biology, University of Southern California, Los Angeles, California 90033

The Ca^{2+}-triggered release of neurotransmitters is mediated by fusion of synaptic vesicles with the plasma membrane. The molecular machinery that translates the Ca^{2+} signal into exocytosis is only beginning to emerge. The soluble *N*-ethylmaleimide-sensitive factor attachment protein receptor (SNARE) proteins syntaxin, SNAP-25, and synaptobrevin are central components of the fusion apparatus. Assembly of a membrane-bridging ternary SNARE complex is thought to initiate membrane merger, but the roles of other factors are less understood. Complexins are two highly conserved proteins that modulate the Ca^{2+} responsiveness of neurotransmitter release. *In vitro*, they bind in a 1:1 stoichiometry to the assembled synaptic SNARE complex, making complexins attractive candidates for controlling the exocytotic fusion apparatus. We have now performed a detailed structural, kinetic, and thermodynamic analysis of complexin binding to the SNARE complex. We found that no major conformational changes occur upon binding and that the complexin helix is aligned antiparallel to the four-helix bundle of the SNARE complex. Complexins bound rapidly ($\approx 5 \times 10^7$ M^{-1} s^{-1}) and with high affinity ($\approx$10 nM), making it one of the fastest protein-protein interactions characterized so far in membrane trafficking. Interestingly, neither affinity nor binding kinetics was substantially altered by Ca^{2+} ions. No interaction of complexins was detectable either with individual SNARE proteins or with the binary syntaxin·SNAP-25 complex. Furthermore, complexin did not promote the formation of SNARE complex oligomers. Together, our data suggest that complexins modulate neuroexocytosis after assembly of membrane-bridging SNARE complexes.

Release of neurotransmitters from presynaptic nerve endings is mediated by fast Ca^{2+}-dependent exocytosis of synaptic vesicles (1). In recent years, many of the molecules responsible for vesicle docking, priming, and fusion have been identified (2–6). Many of these components belong to conserved protein families that operate not only in neuronal exocytosis but also in other intracellular fusion events. This suggests that the basic mechanism of intracellular membrane fusion is conserved (2, 7, 8). The speed of synaptic exocytosis and its tight dependence on Ca^{2+} ions, however, require additional proteins that act upon the basic fusion machine and define its specific features. Among others, those proteins include the soluble and abundant complexins (also referred to as synaphins).

Complexins are two closely related proteins with a molecular mass of ~15,500 Da which do not show significant homologies to other protein families (9). They were first identified by their ability to bind to the synaptic SNARE[1] complex (9–11), which is formed by the proteins synaptobrevin 2 (also referred to as vesicle-associated membrane protein (VAMP) 2), SNAP-25, and syntaxin 1 (12). The core of the synaptic SNARE complex consists of an elongated parallel four-helix bundle structure (13) that can be disassembled by the chaperone-like ATPase NSF in conjunction with α-SNAP (14).

It is currently thought that formation of a membrane-bridging SNARE complex tightly connects the fusing membranes and thus may initiate bilayer merger (15). Complexins may therefore be involved in the control of SNARE function. Their precise role, however, is not yet understood. Neurons lacking both complexins show a decrease in the apparent sensitivity to Ca^{2+}, whereas the spontaneous release is not affected (16). These results suggest that complexins are involved in the Ca^{2+}-dependent triggering step but do not participate in the fusion reaction itself. An activating and late role in exocytosis, presumably independent of Ca^{2+} triggering, was also inferred from peptide injection experiments (17). In contrast, earlier studies, mainly based on microinjection of antibodies and recombinant proteins, seemed to indicate that complexins rather inhibit exocytosis (18). It should be noted, however, that these results are difficult to reconcile with the release properties of neurons lacking complexins (16).

The interactions of complexins with SNAREs have been investigated by several laboratories including our own. We have shown previously that complexins exhibit a central α-helical domain that binds specifically to the assembled synaptic SNARE complex in a 1:1 stoichiometry. The binding site on the SNARE complex appears to involve the surface groove formed by synaptobrevin and syntaxin (19). In another recent study it has been suggested that complexins cause oligomerization of SNARE complexes with the two SNARE motifs of SNAP-25 participating in different complexes (17). Ring-like oligomers

* The costs of publication of this article were defrayed in part by the payment of page charges. This article must therefore be hereby marked "*advertisement*" in accordance with 18 U.S.C. Section 1734 solely to indicate this fact.

§ Present address: Institute for Genetic Medicine and Neurogenetic Institute, Dept. of Biochemistry and Molecular Biology, University of Southern California, Los Angeles, CA 90033.

** To whom correspondence should be addressed: Dept. of Neurobiology, Max Planck Institute for Biophysical Chemistry, Am Fassberg 11, Göttingen D-37077, Germany. Tel.: 49-551-201-1658; Fax: 49-551-201-1499; E-mail: dfassha@mpibpc.gwdg.de.

[1] The abbreviations used are: SNARE, soluble *N*-ethylmaleimide-sensitive factor (NSF) attachment protein (SNAP) receptor; BoNT/C, botulinum neurotoxin C; DTT, dithiothreitol; FRET, fluorescence resonance energy transfer; SNAP-25, synaptosomal associated protein of 25 kDa; TeNT, tetanus neurotoxin.

would be attractive transition structures in membrane fusion, and it has been proposed that complexins oligomerize SNARE complexes in preparation for fusion, thus accelerating the fusion reaction. Such a scenario requires interaction of complexins with either individual SNARE molecules or with partially assembled complexes, which, however, were not observed in our previous study (19).

Taken together, it appears that complexins affect neuroexocytosis via their interaction with SNARE proteins, but it is not clear where exactly in the SNARE cycle they operate and how they affect SNARE function. In particular, it is controversial whether complexins act upon SNAREs only when SNAREs are assembled or whether they influence the assembly and/or the disassembly reaction. Furthermore, it is unclear whether conformational changes are associated upon binding to SNAREs. Obviously, a differentiation between these possibilities is crucial in understanding the molecular role of complexins in controlling membrane fusion. In the present study, we have therefore performed an in-depth analysis of the nature, kinetics, and thermodynamics of the complexin-SNARE interaction using an array of biophysical approaches. EPR and CD spectroscopy inferred that upon binding of complexin to the SNARE complex no major structural changes occur. Fluorescence resonance energy transfer (FRET) measurements indicated that the complexin helix on the surface of the SNARE complex is extended and in an antiparallel orientation to the parallel SNARE complex bundle. No interactions with monomeric SNAREs was found, and no evidence for a role in promoting SNARE oligomers was obtained. Using time-resolved fluorescence anisotropy, we determined association and dissociation rate constants, yielding on-rates in the millisecond range and a high affinity interaction that was confirmed by calorimetric measurements. We conclude that complexins only bind to assembled SNARE complexes with fast kinetics, suggesting that they control a late step in regulated exocytosis.

EXPERIMENTAL PROCEDURES

Materials—Alexa488- and Alexa594-maleimide were purchased from Molecular Probes. Spin label ((1-oxy-2,2,5,5-tetramethylpyrrolinyl-3-methyl)methanthiosulfonate) was a kind gift from Dr. Kalman Hideg (University of Pecs, Hungary). Recombinant protein fragments were derived from cDNAs (rat) encoding for synaptobrevin 2, syntaxin 1A (kindly provided by R. H. Scheller, Stanford, California), SNAP-25A, and complexins I and II (kindly provided by T. C. Südhof, Dallas, Texas).

All proteins were cloned into vectors encoding thrombin-cleavable tagged proteins. The pET-28a vector (Novagen) was used for the following constructs: the cytosolic part of synaptobrevin 2 (residues 1–96), SNAP-25A (1–206) (wild type or all four cysteines substituted by serines (20)), the cytosolic part of syntaxin 1A (1–262), the SNARE motif of syntaxin 1A (180–262), and complexins I and II (1–134). The pET-15b vector (Novagen) was used for the TeNT fragment of synaptobrevin 2 (1–76), the NH_2-terminal (1–83) and COOH-terminal (120–206) fragments of SNAP-25A, and the BoNT/C-fragment of the syntaxin 1A SNARE motif (180–253). Glutathione *S*-transferase-complexin I in pGEX-KG vector (Amersham Biosciences, Inc.) has been described earlier (19).

Generation of Cysteine Mutants—Cysteine mutants of complexin I and II were generated with the QuikChange site-directed mutagenesis kit (Stratagene), using the pET-28a vectors containing wild type complexin I or II as templates. Primers, containing the desired single amino acid mutation, were constructed according to the manufacturer's instructions. First, all natural cysteines in complexins (Cys-105 in complexin I and II and Cys-90 in complexin II) were replaced by serines, and subsequently the following single mutations were introduced in complexin I: D29C, E34C, E35C, E36C, R37C, Q38C, E39C, A40C, L41C, E76C, E81C, and the mutation E39C in complexin II. The correct sequences of all constructs were confirmed by DNA sequencing. The single cysteine mutants of SNAP-25A (Cys-84) and syntaxin 1A (183–262) (Cys-197, Cys-224, Cys-225, Cys-226, and Cys-259) have been described earlier (21).

Protein Expression and Purification—All proteins were expressed according to standard techniques (19–21). After affinity purification on Ni^{2+}-nitrilotriacetic acid-agarose (Qiagen) or glutathione-Sepharose (Amersham Biosciences, Inc.), tags of all constructs were removed by thrombin cleavage during overnight dialysis against standard buffer (20 mM Tris, pH 7.4, 50 mM NaCl, 1 mM DTT, 1 mM EDTA) at 4 °C. All proteins were purified further by ion exchange chromatography using an ÄKTA system (Amersham Biosciences, Inc.).

The following complexes were assembled at 4 °C overnight and again purified by ion exchange chromatography (for details, see Refs. 21–24): the central four-helix bundle domain of the synaptic SNARE complex composed of the SNARE motif of syntaxin 1A (residues 180–262 or 180–253, *i.e.* the BoNT/C fragment), SNAP-25 (residues 1–206), and synaptobrevin (residues 1–96 or 1–76, *i.e.* the TeNT fragment); the syntaxin·SNAP-25 complex composed of two molecules of syntaxin 1A SNARE motif (180–262) and one molecule of SNAP-25 (1–206); the complete cytoplasmic part of the synaptic SNARE complex composed of syntaxin 1A (1–262), SNAP-25 (1–206), and synaptobrevin (1–96); the minimal core complex composed of syntaxin 1A (180–262), SNAP-25 (1–83 and 120–206), and synaptobrevin (1–96).

All proteins and complexes were analyzed by SDS-PAGE and determined to be at least 95% pure. The protein concentration was determined by the Bradford assay (25) and/or by absorption at 280 nm.

Spin Labeling and EPR Measurements—After DTT was removed by dialysis against degassed standard buffer, a 10–20-fold molar excess of the cysteine specific spin label ((1-oxy-2,2,5,5-tetramethylpyrrolinyl-3-methyl)methanthiosulfonate) was added to the various cysteine mutants and allowed to react for at least 2 h on ice. Unreacted spin label was removed by size exclusion chromatography in standard buffer using PD-10 columns (Amersham Biosciences, Inc.).

For assembly of SNARE complexes with spin-labeled complexins, a 1.5-fold molar excess of spin-labeled complexin I was incubated with BoNT/C-truncated SNARE complexes. For assembly of spin-labeled SNARE complexes, TeNT-truncated SNARE complexes containing spin-labeled syntaxins (position 224, 225, or 226) were purified. For assembly with complexin, these complexes were mixed with a 1.5-fold molar excess of unlabeled wild type complexin I. All complexes were allowed to assemble overnight at 4 °C before purification on Mono Q columns using an ÄKTA or SMART system (Amersham Biosciences, Inc.).

Labeled individual proteins and protein complexes were concentrated with Microcons (Millipore), then diluted to final concentrations of 150 or 200 μM and subsequently diluted into sucrose (final concentration 30% (w/w)) to reduce the rotational correlation time. EPR spectra were recorded on a Bruker EMX spectrometer. All spectra were obtained at 2-mW incident microwave power using a field modulation of 1.5 G at 100 kHz and a spectral breadth of 100 G.

Fluorescence Labeling and FRET Measurements—After removal of DTT (see above), single cysteine-containing proteins or protein complexes were incubated with a 10–20-fold molar excess of the fluorescent dye on ice. After at least 2 h, the reaction was stopped by the addition of 10 mM DTT. Labeled proteins were separated from free dye by size exclusion chromatography (Sephadex G-50 superfine material, Amersham Biosciences, Inc.) in standard buffer. The concentration of labeled protein was determined from the absorption at 493 nm (Alexa488) or at 588 nm (Alexa594) using the molar extinction coefficients of the fluorescence dyes. The labeling efficiency is the ratio of labeled and nonlabeled protein, which was determined by the Bradford assay (25).

SNARE complexes with syntaxin mutants containing a single cysteine (position 197 or 259) were formed, purified, and labeled with Alexa594. Because the complex containing syntaxin Cys-259 was not labeled efficiently, syntaxin Cys-259 was labeled before assembly. Complexin I was labeled with Alexa488 at position 29, 39, or 76, and complexin II at position 39. Four different complexin I·SNARE complex complexes, labeled with donor and acceptor dyes, were assembled with a 2-fold molar excess of complexin and purified by ion exchange chromatography (Mono Q, SMART system): 29/197, 76/197, 29/259, and 76/259 (the first number indicates the position of the donor dye in complexin, the second is the position of the acceptor dye in syntaxin).

Spectra were recorded at 25 °C on a Fluorolog-3 with autopolarizers (Jobin Yvon Spex). At 0 degrees vertical excitation (2.0 nm slit width) the emission was monitored at magic angle (2.0 nm slit width). Emission spectra were recorded at 496 nm excitation (range from 500 to 800 nm) of donor/acceptor pairs, acceptor and donor alone, and at 594 nm excitation (600–800 nm) of donor/acceptor pairs and acceptor alone (0.3 μM each in FRET buffer (phosphate-buffered saline, 0.1 mg/ml bovine serum albumin, 0.1% Triton X-100, 0.1 mM EDTA) in 500-μl quartz cuvettes (Hellma).

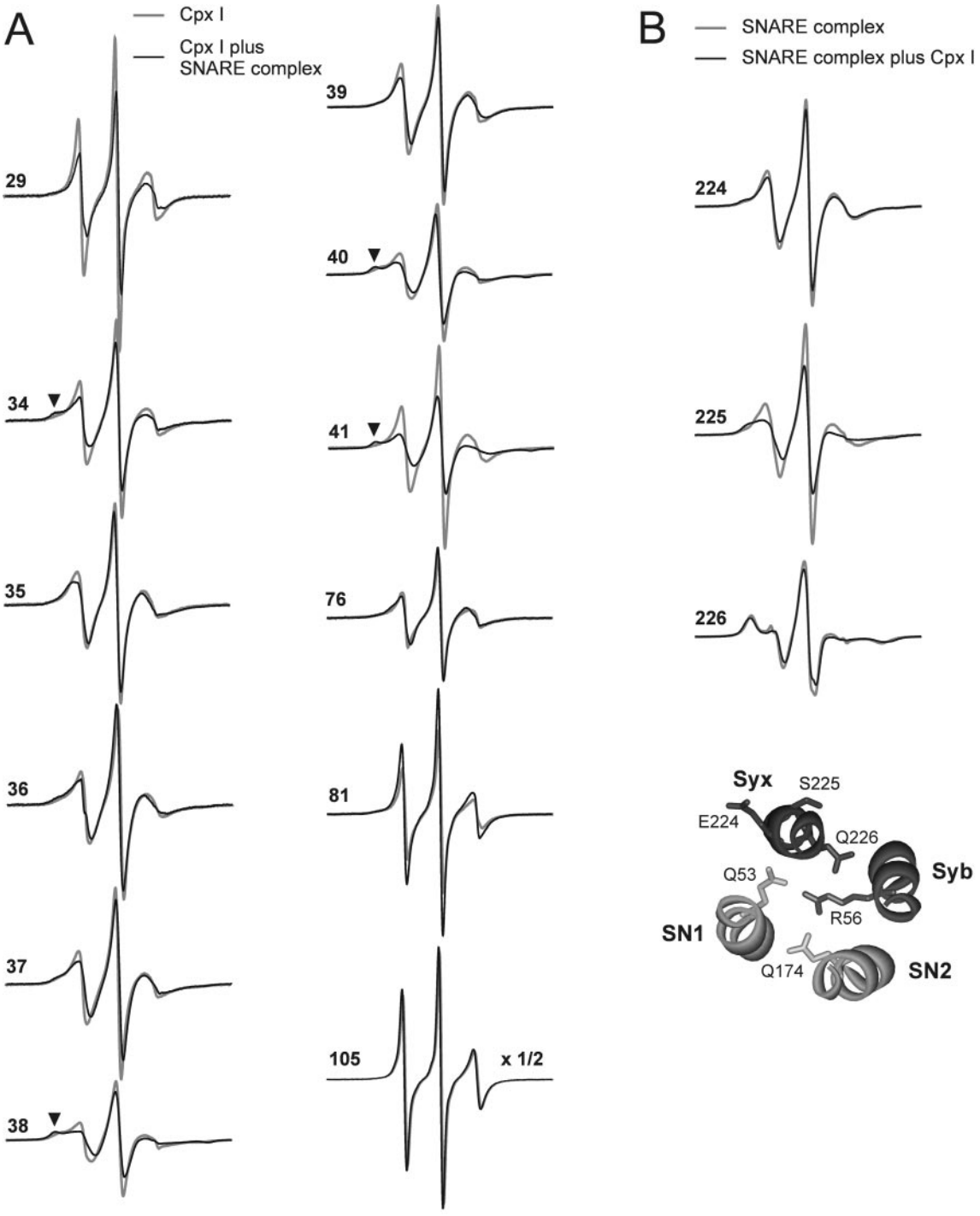

FIG. 1. **Binding of complexin (*Cpx*) to the synaptic SNARE complex monitored by EPR spectroscopy.** *Panel A*, EPR spectra of spin-labeled complexin variants, either free (*gray spectra*) or bound to the synaptic SNARE complex (*black spectra*). Separate spectra were recorded for each labeling position indicated by the *residue number*. The co-complex with the synaptic SNARE complex was purified before spectroscopy. For easier comparison, the spectra for position 105 were multiplied by 1/2. Outer peaks characteristic for immobile side chains were only observed when complexin was bound (*arrowheads*). For details, see "Results." *Panel B*, *top*, EPR spectra of SNARE complexes with spin-labeled syntaxin variants, either free (*gray spectra*) or as purified co-complex with complexin (*black spectra*). Labeling position 226 corresponds to the glutamine in the 0 layer of the complex, whereas positions 224 and 225 are helix surface positions. The scan width was 100 G. *Bottom*, the central region (layers −2 to +1) of the synaptic SNARE complex (13) is depicted as a ribbon diagram (*top view*). Syntaxin residues (224 and 225) and 0 layer residues are shown as *sticks*. *Syx*, syntaxin; *Syb*, synaptobrevin; *SN1*, first helix of SNAP-25; *SN2*, second helix of SNAP-25.

Fluorescence Anisotropy Measurements—Fluorescence anisotropy measurements were performed at 25 °C on a FluoroMax-2 with autopolarizers (Jobin Yvon Spex). Samples were excited with horizontally or vertically polarized light at 488 nm (3–6 nm slit width), and the fluorescence emission was measured at 522 nm (3–6 nm slit width) in horizontal and vertical directions. First, the correction for the instrument response to polarized light (*G* factor) was determined from Equation 1,

$$G = I_{HV}/I_{HH} \quad \text{(Eq. 1)}$$

where I is the fluorescence intensity, and the first subscript letter indicates the direction of the exciting light, and second subscript is the direction of emitted light). Anisotropy (r) was calculated automatically by the software of the instrument using Equation 2.

$$r = (I_{VV} - G \times I_{VH})/(I_{VV} + 2 \times G \times I_{VH}) \quad \text{(Eq. 2)}$$

TABLE I
Line widths of EPR spectra

Labeled position in Cpx I[a]	Line width, Cpx I alone	Line width, Cpx I plus SNARE complex
29	2.10	2.30
34	2.49	2.83
35	2.59	3.13
36	2.64	3.08
37	2.59	3.27
38	3.27	3.96
39	2.59	2.83
40	2.98	3.52
41	2.64	3.81
76	2.25	2.54
81	2.20	2.05
105	1.91	1.91
Labeled position in syntaxin	**Line width, SNARE complex alone**	**Line width, SNARE complex plus Cpx I**
224	2.88	2.93
225	3.08	3.86
226	4.69	5.37

[a] Cpx, complexin.

To investigate the interaction of complexin, changes in the anisotropy of Alexa488-labeled complexin I (Cys-39) were measured in polystyrene cuvettes (Sarstedt). To 100 nM labeled complexin in FRET buffer, 1 μM individual SNARE proteins or SNARE complexes were added. Samples were mixed throughout the experiment by a magnetic stirrer. Data points were recorded every 10 s.

For kinetics of SNARE complex assembly, a mixture of 500 nM synaptobrevin (1–96), and syntaxin (180–262) was added after 400 s to a mixture of 5 nM Alexa488-labeled SNAP-25 (Cys-84) and 500 nM complexin I or II. FRET buffer (see above) or Ca^{2+} buffer (20 mM Tris, pH 7.4, 100 mM NaCl, 0.1% Triton X-100, 0.1 mg/ml bovine serum albumin, 1 mM Ca^{2+}) was used. Data points were recorded every 20 s.

Stopped-flow Measurements—Experiments of binding and dissociation kinetics of complexin and the SNARE complex were performed using the stopped-flow instrument SX.18MV (Applied Photophysics) with a 20-μl optical detection cell. Alexa488-labeled samples were excited at 490 nm (9.2 nm slit width) and OG530 cut-off filters (Schott) were used in both fluorescence polarization detection paths (T format). The *G* factor (see above) of the instrument was measured automatically by the system at the beginning of every experiment. Fluorescence anisotropy and fluorescence total intensity data were obtained "on the fly" from the parallel and perpendicular channel data. Fluorescence total intensity (S) was calculated as

$$S = I_{VV} + 2 \times G \times I_{VH} \quad \text{(Eq. 3)}$$

(for abbreviations and formula for fluorescence anisotropy, see above). For each injection, 1,000 data points were recorded in a time window of either 0.5, 1, 2, 20, or 50 s (chosen to obtain optimal resolution of the ascending or descending phase) at 25 °C.

For the determination of the on-rates 100 nM Alexa488-labeled complexin I or II (position 39) was mixed with BoNT/C-truncated SNARE complex (200–600 nM) in FRET buffer (see above) or with 400 nM BoNT/C-truncated SNARE complex in Ca^{2+} buffer (see above) in the stopped-flow apparatus. Multiple kinetic runs (n = 21–40) were averaged to obtain adequate signal:noise ratios.

Global analysis of the kinetic traces of the fluorescence anisotropy and the fluorescence total intensity was done using a home-written analysis software based on the theoretical approach described previously (26). The two kinetic traces were fitted simultaneously by numerically solving the system of differential equations, describing a bimolecular second order reaction: A + B ↔ C. The two of three species (B and C) were characterized by their quantum yield (q_i) and their anisotropy (r_i) level. The observed fluorescence total intensity was calculated as

$$S(t) = \Sigma x_i(t) \times q_i \quad \text{(Eq. 4)}$$

where $x_i(t)$ is the concentration of species i at time t. The observed fluorescence anisotropy was calculated as in Equation 5.

$$r(t) = (\Sigma x_i(t) \times r_i \times q_i)/(\Sigma x_i(t) \times q_i) \quad \text{(Eq. 5)}$$

The fitting procedure provides the on-rate of the reaction being analyzed, the two quantum yields (q_i) and the two anisotropy levels (r_i).

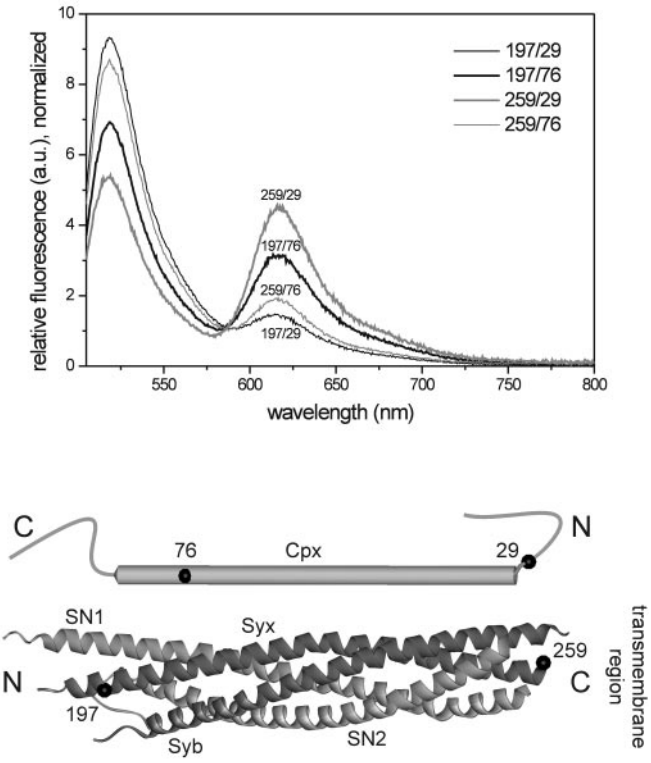

FIG. 2. **FRET measurements indicate that complexin is aligned antiparallel to the α-helices of the synaptic SNARE complex.** *Top panel*, emission spectra, normalized to the areas under the graphs, for different SNARE·complexin complexes labeled with Alexa488 (donor) and Alexa594 (acceptor) (λ_{ex} = 496 nm). The *numbers* indicate the side chain position of the donor dye in complexin and of the acceptor dye in syntaxin, respectively. A high FRET efficiency was observed for the pairs 197/76 and 259/29, visible by a decrease in donor fluorescence and a corresponding increase in acceptor fluorescence, whereas less FRET was observed for the pairs 197/29 and 259/76. *Bottom panel*, relative orientation of the labeling positions (*black balls*) for syntaxin and for complexin as implied by the FRET measurements. The α-helical region of complexin (residues 29–86, as mapped by NMR (19)) is drawn as a *tube*, the structure of the synaptic SNARE complex (13) is depicted as a *ribbon* diagram. *Cpx*, complexin; *Syx*, syntaxin; *Syb*, synaptobrevin; *SN1*, first helix of SNAP-25; *SN2*, second helix of SNAP-25; *N*, NH_2 terminus; *C*, COOH terminus.

TABLE II
Calculated FRET efficiencies and distances between donor/acceptor molecules

FRET efficiencies and distances between Alexa488-labeled complexin (donor) and Alexa594-labeled syntaxin (acceptor) as part of the SNARE complex were calculated by the method of Jares-Erijman and Jovin (36). The labeling efficiencies of the donor in double labeled complexes were taken into account (95% for complexin 29-syntaxin 197, 100% for 76–197, 82% for 29–259, and 98% for 76–259). Note that because of the length of the linker regions of the fluorescent dyes an error for the distances has to be considered.

Donor, Alexa488		Acceptor, Alexa594		FRET efficiency	Distance
				%	Å
Cpx[a]	C29	Syx[b]	C197	12	75
Cpx	C76	Syx	C197	46	55
Cpx	C29	Syx	C259	83	41
Cpx	C76	Syx	C259	42	57

[a] Cpx, complexin.
[b] Syx, syntaxin.

Interestingly, in contrast to all other measurements, upon binding of complexin II to the SNARE complex in the presence of Ca^{2+} no change in fluorescence total intensity was detected. Thus, in this case no simultaneous analysis of fluorescence anisotropy and fluorescence total intensity was possible, and the on-rate of this reaction was determined

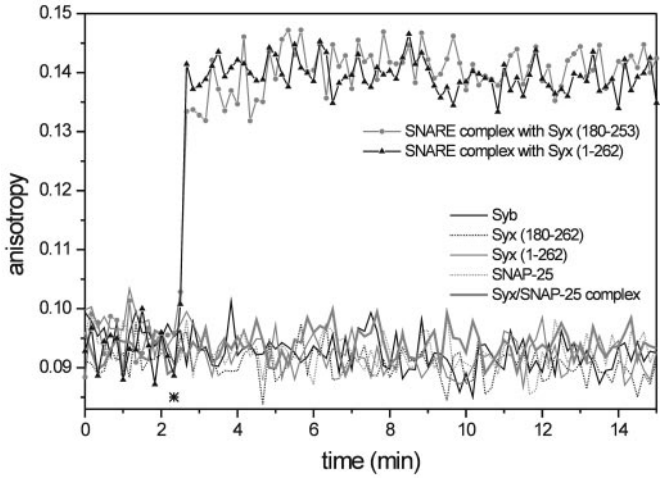

FIG. 3. **Binding of complexin to the synaptic SNARE complex monitored by fluorescence anisotropy.** Binding was observed as change in fluorescence anisotropy of 100 nM complexin I, labeled at position 39 with Alexa488. Excess amounts of individual SNARE proteins and SNARE complexes were added (final concentration 1 μM, *asterisk*). The addition of ternary SNARE complexes, containing either the SNARE motif of syntaxin (*Syx 180–253*) or the entire cytoplasmic region (*Syx 1–262*) led to rapid increases in anisotropy. No change in anisotropy was detected upon addition of either SNARE monomers or binary syntaxin·SNAP-25 complex.

by analyzing only the fluorescence anisotropy using the software mentioned above. Because of identical values of quantum yields (q_i) of both B and C species, the expression of the observed fluorescence anisotropy can be transformed in this case to the form

$$r(t) = \Sigma x_i(t) \times (r_i/b) \quad \text{(Eq. 6)}$$

where $b = \Sigma\, x_i(t) = \text{const.}$; b is the initial concentration of species B. It is important to note that here summation is performed only over the species, which contribute to the fluorescence signal.

For the determination of the off-rates an equimolar mixture of 100 nM Alexa488-labeled complexin I or II and SNARE complex (containing syntaxin 180–253, preincubated for 1 h at 25 °C) was mixed with 10 μM unlabeled complexin I or II in FRET buffer in the stopped-flow apparatus. Again, 1,000 data points were recorded as described above (n = 15). The data were analyzed by fitting the averaged fluorescence total intensity data with a single-exponential function

$$y = a + b \times e^{-c \times t} \quad \text{(Eq. 7)}$$

where y is the fluorescence total intensity or the anisotropy and t the time using Microcal Origin 5.0. Averaged fluorescence anisotropy values were then multiplied with the fitted curve. The corresponding data set was fitted again with the single-exponential function yielding the off-rate (c).

Isothermal Titration Calorimetry—Isothermal titration calorimetry was performed on a MCS instrument (Microcal) at 25 °C. Samples were dialyzed against degassed Tris buffer (20 mM Tris, pH 7.4, 100 mM NaCl, 1 mM DTT, and either 1 mM EDTA or 1 mM Ca^{2+}) or phosphate buffer (20 mM sodium phosphate, pH 7.4). The protein concentration of the SNAREs or SNARE complexes in the cell was 5 μM. 70–100 μM complexins were added in 7- or 10-μl injections. The data were analyzed with Microcal Origin 5.0 using a single-site binding model, yielding the equilibrium association constant K_a, the enthalpy of binding ΔH_a, and the stoichiometry N.

CD Spectroscopy—Far UV-CD spectra were recorded in 20 mM sodium phosphate buffer, pH 7.4, in a tandem cell (2 × 4.375 mm path length, Hellma). 1.5 μM complexin I was added to one chamber and 1.5 μM minimal core complex to the other chamber. First, the noninteracting spectrum of both proteins (sum of both, without mixing) was measured. After mixing and a 1-h incubation, the interacting spectrum was recorded.

For SNARE assembly kinetics, about 1.5 μM individual SNARE proteins were mixed in 20 mM Tris, pH 7.4, 100 mM NaCl, and the ellipticity at 220 nm was recorded as a function of time. Because SNAP-25 and synaptobrevin do not interact, the reaction was started by the addition of syntaxin (180–262) to a mixture of SNAP-25 and synaptobrevin (1–96) with or without 1.6 μM complexin II.

Formation of SDS-resistant SNARE Complexes—Formation of SDS-resistant SNARE complexes in the presence of complexin was monitored upon SDS-PAGE (27) followed by Coomassie Blue staining as described previously (19). About 10 μM synaptobrevin (1–96), wild type or cysteine-free SNAP-25 (1–206), and syntaxin 1A (1–262) was incubated in the presence of increasing amounts of complexin II for at least 16 h at 4 °C in incubation buffer (20 mM Tris, pH 7.4, 50 mM NaCl, 1 mM DTT, and 1 mM EDTA.) When wild type recombinant SNAP-25 that contained all four cysteines was used, the incubation was carried out in

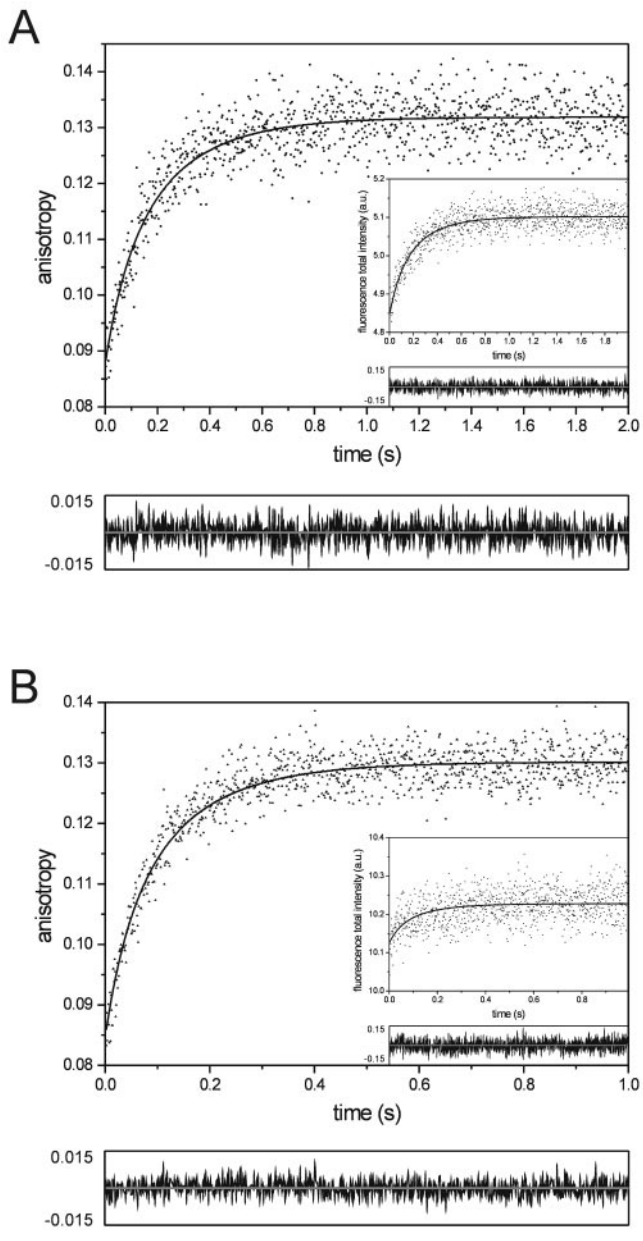

FIG. 4. **Kinetics of complexin binding measured by fluorescence anisotropy in a stopped-flow apparatus.** Complexins, labeled at position 39 with Alexa488, were mixed with purified synaptic SNARE complexes in a stopped-flow apparatus. Illustrated are the experiments in which 200 nM SNARE complex was mixed with 100 nM labeled complexin. Averaged data points from several kinetic traces, in which the fluorescence anisotropy and the fluorescence total intensity were recorded simultaneously, are shown for complexin I (*panel A*, n = 21) and complexin II (*panel B*, n = 37). The changes in fluorescence total intensity (*insets*) and fluorescence anisotropy were fitted using a numerical approach (see "Experimental Procedures"). Residuals of the fitted curves are shown at the *bottom* of the graphs. Note that the amplitude for the change in fluorescence total intensity for complexin II is smaller than for complexin I, probably because of a slightly different molecular environment of the dye after binding. Note that the time scales in *panels A* and *B* are different to resolve the different binding kinetics of complexin I and complexin II optimally.

TABLE III
Association rate constants for the interaction of complexin with the SNARE complex

The association rate constants (k_{on}) were calculated from n recordings as described under "Experimental Procedures." Steady-state fluorescence anisotropy values ($r_{free\ protein}$ and $r_{bound\ protein}$) from the calculations are shown. Buffers contained either 0.1 mM EDTA or 1 mM Ca^{2+} (asterisks).

100 nM, Alexa488-labeled (pos. 39)	SNARE complex	k_{on}	n	r_{free}	r_{bound}
	nM	$M^{-1}\ s^{-1}$			
Cpx[a] I	200	3.0×10^7	21	0.088	0.136
	400	3.2×10^7	29	0.089	0.134
	600	3.3×10^7	35	0.088	0.134
Cpx II	200	6.5×10^7	37	0.085	0.130
	400	6.0×10^7	40	0.086	0.131
	600	6.0×10^7	39	0.084	0.131
Cpx I*	400	3.0×10^7	24	0.093	0.151
Cpx II*	400	7.9×10^7	32	0.074	0.140

[a] Cpx, complexin.

the presence or absence of 1 mM DTT. Then, before mixing, all proteins were dialyzed against incubation buffer with or without DTT. After incubation, SDS sample buffer (final concentrations: 62.5 mM Tris, pH 6.8, 3% SDS, 10% glycerol, 3.3% β-mercaptoethanol) was added, and samples were separated without heating on 15% polyacrylamide gels.

RESULTS

Characterization of Complexin Binding to SNARE Complexes Using EPR and FRET Spectroscopy—In our previous study, a central region of complexin was shown to be sufficient for SNARE complex binding. NMR spectroscopy revealed that in individual complexin this region is α-helical. To analyze the structure and orientation of the interacting helical region upon binding, we now used EPR spectroscopy. In this procedure, individual side chains are spin-labeled, allowing for a detailed assessment of side chain mobility of the free *versus* bound protein.

Complexin I contains a natural cysteine at position 105. In addition to wild type complexin I, we generated a series of cysteine variants, in which Cys-105 was replaced with serine, and single new cysteines were introduced each at positions 29, 76, and 81. In addition, to monitor for α-helical periodicity we mutated each position between residues 34 and 41 in the binding region of complexin I to a cysteine. All variants were purified and labeled with the cysteine-specific spin label (1-oxy-2,2,5,5-tetramethylpyrrolinyl-3-methyl)methanthiosulfonate.

EPR spectra were recorded of each of the variants either as individual proteins (Fig. 1*A*, *gray spectra*) or in association with unlabeled SNARE complexes (consisting of the SNARE motifs of synaptobrevin 2, SNAP-25A, and syntaxin 1A; *black spectra*). To minimize self-induced oligomerization of SNARE complexes, we used SNARE complexes that contained a carboxyl-terminally truncated syntaxin 1A (Syx 180–253; for details, see Ref. 21).

As can be seen from Fig. 1*A* and Table I, the spectra obtained for the free complexin variants labeled at positions 34–76 were similar to each other. Their amplitudes and central line widths concur with the formation of secondary structure (for further information, see Refs. 28–31). Previous data indicated that this part of complexin is α-helical even though the protein is monomeric (19). Typically, secondary structure can be detected by EPR spectroscopy based on the periodicity of buried and surface residues. No periodicity was observable (Fig. 1*A*), however, probably because the complexin helix does not form tertiary contacts. Interestingly, the central line widths were smaller than those observed for helix surface positions in the SNARE complex (21). This appears to reflect the higher dynamics of the protein backbone of complexin. The labeling positions adjacent to this central region (Cys-29, Cys-81, and Cys-105) resulted in sharp and narrowly spaced peaks typical for a high degree of mobility. This suggests that these residues do not exhibit a stable secondary structure. These data are in excellent agreement with our previous NMR analysis, which indicated that the stretch from 29 to 86 is mostly α-helical (19).

TABLE IV
Dissociation rate constants for the interaction of complexin with the SNARE complex

The dissociation rate constants (k_{off}) were calculated from n recordings as described under "Experimental Procedures."

100 nM, Alexa488-labeled Cpx[a] (pos. 39)	Unlabeled, 10 μM	k_{off}	n
		s^{-1}	
Cpx I · SNARE complex	Cpx I	3.1×10^{-1}	15
Cpx II · SNARE complex	Cpx II	4.1×10^{-1}	15

[a] Cpx, complexin.

When these spectra were compared with those obtained when complexin is bound to the SNARE complex, we noted a significant decrease in mobility for all labeling positions between residues 29 and 41 (Fig. 1*A*, *black lines*). This is evident, for instance, by an increase in the central line width (Table I). Thus binding of complexin to the SNARE complex induced new packing interactions. Furthermore, outer peaks characteristic for immobile side chains were observed for residues 34, 38, 40, and 41 (see *arrowheads* in Fig. 1*A*). The periodicity of these immobile side chains suggests that a new contact is formed at one side of the complexin helix. This strengthens the view that the complexin helix is aligned along the surface of the SNARE complex. Only minor changes, however, were observed in the spectra obtained for positions 76, 81, and 105, which are outside of the central binding region.

Next we labeled syntaxin residues 224, 225, and 226 and recorded EPR spectra of SNARE complexes (containing TeNT-truncated synaptobrevins to minimize self-oligomerization of SNARE complexes, see Ref. 21) alone and in combination with unlabeled complexin I (Fig. 1*B*). We have shown previously that swapping residues 214–225 between syntaxin 1A and syntaxin 4 strongly decreased complexin binding, suggesting that this stretch is in contact with complexin. In the SNARE complex, residues 224 and 225 are on the surface of the syntaxin helix and are oriented toward the helices of the NH_2-terminal part of SNAP-25 and synaptobrevin, respectively (Fig. 1*B*, *bottom*). Yet, they are free of contact. Residue 226 is buried in the interior of the helix bundle and interacts with corresponding residues of the other helices as part of the 0 layer (13). Accordingly, the EPR spectra of positions 224 and 225 were typical for helix surface, whereas the spectrum of position 226 had a strong immobile component (for details, see Ref. 21). In the presence of complexin a significant decrease in mobility was observed for position 225, suggesting that this residue is in direct contact with complexin. As mentioned above, the syntaxin residue 225 projects into direction of the neighboring synaptobrevin helix (Fig. 1*B*, *bottom*). Interestingly, no significant change was observed for position 224, which is oriented toward the first SNAP-25 helix. This is in agreement with our earlier finding according to which complexin binds into the groove between syntaxin and synaptobrevin (19).

To determine the relative orientation of complexin to the SNARE complex, we used FRET, which allows for an approximate determination of distances. Complexin I was labeled either at position 29 or at position 76 with the fluorescence donor Alexa488. Furthermore, we prepared SNARE complexes that were labeled with acceptor dye Alexa594 at syntaxin position 197 or 259 (for the relative orientation of the labeling positions, see Fig. 2). Fig. 2 shows the emission spectra that were obtained upon donor excitation for each combination of labeling positions. FRET is visible by a decrease in donor and a

TABLE V
Equilibrium dissociation rate constants for the interaction of complexin with the SNARE complex

The equilibrium dissociation rate constants (K_d) were calculated from k_{off}/k_{on} (mean values; see Tables IV and III, respectively), yielding also the free energy of binding ($\Delta G_a = -RT \ln (1/K_d)$).

Average	k_{on}	k_{off}	K_d	ΔG_a
	$M^{-1}\ s^{-1}$	s^{-1}	M	$kcal\ mol^{-1}$
Cpx[a] I	3.1×10^7	3.1×10^{-1}	10×10^{-9}	−11
Cpx II	6.6×10^7	4.1×10^{-1}	6.2×10^{-9}	−11

[a] Cpx, complexin.

corresponding increase in acceptor fluorescence. The strongest degree of FRET was observed for the combinations complexin 29-syntaxin 259 and complexin 76-syntaxin 197 (see also Table II). In contrast, very little FRET was observed between complexin 29 and syntaxin 197. This suggests that the binding region of complexin is antiparallel to the alignment of the helices in the SNARE complex, probably forming an extended α-helix. Interestingly, the distance of complexin 76 to syntaxin 259 is in the same range as to syntaxin 197. Because this position does not interact directly with the surface of the SNARE complex (see Fig. 1*A*), it cannot be excluded that the COOH-terminal part of the helical region of complexin is somewhat bent away from the SNARE complex.

Kinetics of Complexin Binding and Dissociation—In the next set of experiments, we determined the association and dissociation rates of complexin binding to the synaptic SNARE complex using fluorescence anisotropy. For this purpose we labeled complexin I and complexin II at position 39 with the dye Alexa488. Position 39 was chosen because it is part of the interacting region but is not buried (see Fig. 1*A*), making it unlikely that the kinetic parameters are affected by the presence of the dye molecule. As expected, a large and rapid increase in fluorescence anisotropy was observed when labeled complexins were incubated with the core of the synaptic SNARE complex. This indicates that binding led to an increase of rigidity near the labeled residue (Fig. 3). A similar increase in anisotropy was observed when a synaptic SNARE complex containing the entire cytoplasmic region of syntaxin was added to complexin. No increase in anisotropy, however, was seen with any of the individual SNARE proteins. This supports our previous observation that complexin only binds to assembled SNARE complexes (19). Similarly, mixing of complexins with the preformed syntaxin·SNAP-25 complex did not lead to an increase in anisotropy. This complex consists of a four-helix bundle similar to the synaptic SNARE complex but with a second syntaxin helix occupying the binding site of synaptobrevin (21, 22, 32). Apparently, this exchange disrupts the binding of complexin to the surface of the synaptic SNARE complex.

The rapid increase of anisotropy upon complexin binding prompted us to use a stopped-flow procedure for the determination of the association rates. Complexins (final concentrations 100 nM) and synaptic SNARE complex (with the BoNT/C-truncated SNARE motif of syntaxin, see above; final concentration 200, 400, or 600 nM) were mixed in a stopped-flow apparatus. For each recording, 1,000 data points were obtained (fluorescence anisotropy and fluorescence total intensity) in a time window of either 0.5, 1, or 2 s (chosen to obtain optimal resolution of the ascending phase). Fig. 4 shows the data for complexin I (Fig. 4*A*) and complexin II (Fig. 4*B*), mixed with 200 nM SNARE complex. From the fits we obtained the association rate constants for binding of complexin I and II to the synaptic SNARE complex: $3.1 \times 10^7\ M^{-1}\ s^{-1}$ and $6.6 \times 10^7\ M^{-1}\ s^{-1}$, respectively. Interestingly, in the presence of Ca^{2+} no substantial changes in the on-rates but a slight acceleration for complexin II were observed (Tables III and V).

For the determination of dissociation rates, SNARE complex was first incubated with an equimolar amount of labeled complexin and then mixed with a 100-fold molar excess of unlabeled complexin in the stopped-flow apparatus. Dissociation was monitored by the decrease of anisotropy associated with the displacement of labeled complexin from the complex. Again, 1,000 data points were obtained in time windows of 20 or 50 s (Fig. 5). The off-rates for complexin I and II were 0.31 s^{-1} and 0.41 s^{-1}, respectively (Tables IV and V).

Several conclusions can be drawn from these data. First, binding is very fast and occurs on a millisecond time scale, *i.e.* compatible with a function in a fast reaction sequence as required for neuronal exocytosis. Such fast reactions imply that no major structural changes can occur during binding. Nevertheless, we cannot exclude that additional, though small, conformational changes follow the first contact because we monitored association/dissociation by changes of the fluorescence anisotropy of a single labeled residue only. Second, the equilibrium binding constants for both complexins were very similar, although complexin II bound and dissociated somewhat faster than complexin I. Third, addition of Ca^{2+} did not affect the association rate extensively, suggesting that binding is not altered significantly by the presence of Ca^{2+} ions.

Determination of the Thermodynamic Parameters of Complexin Binding Using Microcalorimetry—The thermodynamics of the complexin·SNARE complex interaction was measured by isothermal titration calorimetry. The results of typical isothermal titration calorimetry experiments at 25 °C are shown in Fig. 6. Binding of complexins to the synaptic SNARE complex was an exothermic reaction, and thus the binding enthalpy was favorable. No enthalpically detectable binding was observed, however, when complexin II was mixed with the SNARE motif of syntaxin or the syntaxin·SNAP-25 complex (Fig. 1*B*), once again confirming that binding is restricted to the assembled SNARE complex (Ref. 19 and see above).

Curve fitting of the binding isotherm of the complexin·SNARE complex interaction showed that binding occurred with a 1:1 stoichiometry with no detectable secondary binding (Table VI). The equilibrium dissociation constants for both complexins obtained by the fit were largely similar (Table VI) and agree with the constants obtained by the kinetic analysis. Because isothermal titration calorimetry only yields accurate equilibrium constants for affinities above ≈ 10 nM and the investigated binding is very tight, the equilibrium dissociation constants calculated from the on- and off-rate determinations are probably more reliable.

When complexin I and II were mixed with a synaptic SNARE complex containing the entire cytoplasmic region of syntaxin, similar thermodynamic parameters were found (Table VI). This confirms that the binding region for complexins is limited to the surface of the four-helix bundle of the synaptic SNARE complex (19). It also excludes that the NH_2-terminal domain of syntaxin, which is not part of the central SNARE helix bundle, interferes with binding of complexin.

Interestingly, a large difference in the apparent enthalpies of the interaction of complexin I and II with the synaptic SNARE complex was observed ($\Delta\Delta H \approx -14$ kcal mol^{-1}, in Tris buffer). The apparent binding enthalpy is composed mainly of solvent reorganizations and direct noncovalent bonds at the binding interface. Consequently, the enthalpic difference between complexin I and II could not directly be attributed to differences in the side chains participating in the binding. The difference in enthalpy of the two complexins was only weakly correlated to a change in ΔG, a common thermodynamic behavior that is thought to reflect an important role of compensating enthalpy and entropy contributions of water to the binding process (33).

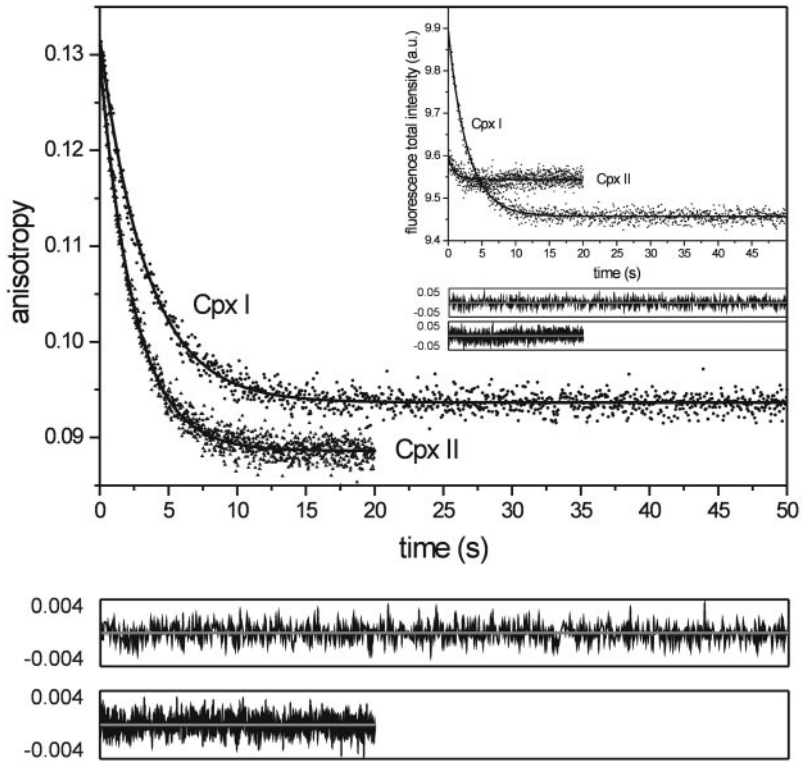

FIG. 5. **Dissociation kinetics of complexin, measured by stopped-flow fluorescence anisotropy.** An equimolar mixture of 100 nM SNARE complex and Alexa488-labeled complexin I or II (labeled at position 39) was mixed with 10 μM unlabeled complexin I or II, respectively. Displacement of labeled complexin from the SNARE complex by its unlabeled counterpart is accompanied by a decrease in fluorescence anisotropy. The averaged data from 15 experiments, fluorescence anisotropy, and fluorescence total intensity (*inset*) and the fitted curves (*black lines*) are plotted for complexin I (*circles*) and II (*triangles*). Residuals of the fitted curves are shown at the *bottom* of the graphs. For details, see "Experimental Procedures."

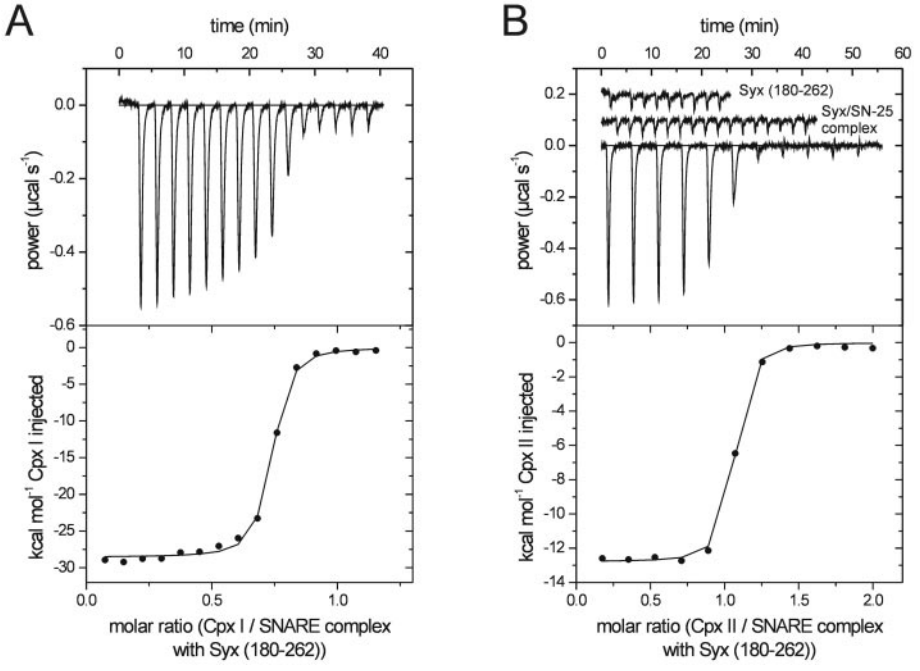

FIG. 6. **Thermodynamics of the complexin·SNARE complex interaction.** Calorimetric titration of complexin I (*panel A*) or complexin II (*panel B*) to the core of the synaptic SNARE complex in 20 mM sodium phosphate, pH 7.4, at 25 °C. The *top panels* show base-line corrected raw data in power *versus* time. The area under each spike is proportional to the heat produced at each injection. The *lower panels* display integrated areas normalized to the amount of complexin injected (kcal mol^{-1}) *versus* molar ratio of complexin to the SNARE complex. The *solid line* is the best fit to the data for a single binding site model using a nonlinear least squares fit. Different binding enthalpy changes (ΔH) were observed for complexin I ($\approx$29 kcal mol^{-1}) and complexin II ($\approx$13 kcal mol^{-1}), the equilibrium dissociation constants (K_d) were 8.5 nM and 15 nM, respectively. No change was observed upon injection of complexin II to the syntaxin SNARE motif or the binary syntaxin·SNAP-25 complex (*panel B*, *upper traces*), confirming that complexin binds only to the assembled ternary SNARE complex. *Syx*, syntaxin; *SN-25*, SNAP-25.

Interestingly, complexin I bound more slowly to the SNARE complex than complexin II (Fig. 4 and Tables III and V). It seems possible that this reflects larger solvent reorganizations upon binding as apparent in larger enthalpy in complexin I than in complexin II.

Notably, a difference in the binding enthalpies for complexin II was observed in phosphate buffer (≈ -12.8 kcal mol^{-1}) and Tris buffer (≈ -17.0 kcal mol^{-1}) at pH 7.4 (Table VI). The heat of ionization is different for phosphate (-0.8 kcal mol^{-1}) and Tris (-11.4 kcal mol^{-1}) (34). Because ΔH in phosphate buffer is less exothermic, it may be concluded that the difference in the observed binding enthalpies is caused by a partial release of a proton. No protonation effect was observed for complexin I (Table VI), making it likely that the proton is not released from the SNARE complex. Because complexin I does not contain a histidine residue in the binding region (although the vector derived residues GSH remained attached to both complexins after thrombin cleavage), a potential candidate responsible for release of a proton from complexin II is the single histidine at position 52 (tyrosine in complexin I). Possibly, the pK_a of histidine 52 is shifted from 6.5 to neutral pH upon binding.

Influence of Complexin on SNARE Complex Formation—The data described so far show that complexin binding to the ternary SNARE complex is very rapid. Furthermore, binding appears to be exclusive for the assembled SNARE complex be-

TABLE VI

Thermodynamic parameters of complexin binding determined by isothermal titration calorimetry

SNARE complexes contained either the syntaxin SNARE motif (180–262) or the entire cytoplasmic region (1–262) of syntaxin (asterisks). Different buffers were used: 20 mM Tris, pH 7.4, 100 mM NaCl, 1 mM DTT, and either 1 mM EDTA (Tris/EDTA) or 1 mM Ca^{2+} (Tris/Ca^{2+}) or 20 mM sodium phosphate buffer, pH 7.4 (phosphate). The equilibrium dissociation constants ($K_d = 1/K_a$), enthalpies of binding (ΔH_a), and the stoichiometries (N) were determined with Microcal Origin 5.0 using a single site binding model (upper section). Mean values of the equilibrium dissociation constants are shown in the lower section. The free energy of binding (ΔG_a) was calculated from the relation $\Delta G_a = -RT \ln (1/K_d)$.

Reaction with SNARE complex	Buffer	K_d	ΔH_a	N
		M	*kcal mol*$^{-1}$	
Cpx I	Phosphate	$(8.5 \pm 1.5) \times 10^{-9}$	-28.6 ± 0.2	0.71
Cpx I	Tris/EDTA	$(2.1 \pm 0.4) \times 10^{-8}$	-31.4 ± 0.3	0.88
Cpx I	Tris/Ca^{2+}	$(2.1 \pm 0.7) \times 10^{-8}$	-30.6 ± 0.5	0.86
Cpx II	Phosphate	$(1.5 \pm 0.4) \times 10^{-8}$	-12.8 ± 0.1	0.99
Cpx II	Tris/EDTA	$(2.4 \pm 0.4) \times 10^{-8}$	-18.0 ± 0.1	0.99
Cpx II	Tris/Ca^{2+}	$(4.3 \pm 0.9) \times 10^{-8}$	-16.3 ± 0.2	0.88
Cpx I*	Tris/EDTA	$(2.5 \pm 0.5) \times 10^{-8}$	-29.9 ± 0.3	0.85
Cpx II*	Tris/EDTA	$(2.0 \pm 0.3) \times 10^{-8}$	-16.8 ± 0.1	0.94
Average		K_d	ΔG_a	
		M	*kcal mol*$^{-1}$	
Cpx I		1.9×10^{-8}	-11	
Cpx II		2.6×10^{-8}	-10	

cause no interaction was observable with individual SNAREs. These observations, however, do not exclude that complexins influence the rate or the structural features of SNARE assembly. For instance, it has been proposed recently that complexins catalyze the formation of higher order SNARE oligomers, in which the two SNARE motifs of SNAP-25 are part of different complexes (17). Obviously, it is of prime importance for an understanding of complexin's function to know whether complexins act after SNAREs have assembled or whether they regulate the assembly reaction itself. For these reasons, we have investigated the effect of complexins on the rate of SNARE complex formation and whether they promote oligomer formation.

SNARE assembly is accompanied by a large increase in α-helical content (22), whereas the addition of complexin I to an assembled SNARE complex was not associated with a significant conformational change (Fig. 7*A*, *inset*). Hence, we monitored SNARE complex formation by CD spectroscopy. SNARE assembly was slow with a half-life of about 525 s at a protein concentration of 1.5 μM (Fig. 7*A*). Similar kinetic behavior was observed when the incubation was carried out in the presence of 1 mM Ca^{2+} (data not shown). The addition of complexin II to the assembly reaction led to an (overall) increase in α-helical content because complexins are partially α-helical in solution (Ref. 19 and Fig. 1*A*). Nevertheless, no significant change in the rate of association was detected in the presence of complexin (half-life of about 534 s).

As an independent approach to monitor SNARE complex formation, we measured the increase in fluorescence anisotropy of a SNAP-25 variant labeled with Alexa488 at Cys-84. We added a mixture of synaptobrevin and the SNARE motif of syntaxin (500 nM) to 5 nM labeled SNAP-25. Again, no change in the rate of SNARE complex formation was observed when 500 nM complexin I or complexin II was present (Fig. 7*B*). Also, the same reaction rates were observed regardless of whether the incubation was carried out in the presence of 0.1 mM EDTA (Fig. 7*B*) or 1 mM Ca^{2+} (Fig. 7*C*).

Finally, we examined whether complexin induces the formation of higher order oligomers of SNARE complexes. For this purpose, increasing concentrations of purified complexin were incubated with 10 μM recombinant synaptobrevin, syntaxin 1, or SNAP-25. Complex formation was monitored by SDS-PAGE followed by Coomassie Blue staining. As shown in Fig. 8*A*, the presence of complexin II did not promote the formation of SNARE complex oligomers. To exclude that the absence of cysteines in our constructs is responsible for this lack of oligomerizing activity, the experiments were repeated using a wild type SNAP-25 construct containing the four native cysteines in the loop region of SNAP-25. Again, complexin did not induce oligomer formation regardless of whether the experiment was carried out in the presence of reducing agents (Fig. 8*B*). A further increase of the complexin:SNARE ratio (up to 60-fold) did not change this result (data not shown). Moreover, neither CD nor fluorescence spectroscopy indicated that complexins induce oligomerization of SNARE complexes. We conclude that complexins have no effect on the SNARE assembly reaction.

DISCUSSION

In the present study, we used a combination of biophysical techniques to characterize the interaction of complexins with the synaptic SNARE complex. Complexins only bind to assembled SNARE complexes and do not influence the SNARE assembly reaction in any way. Our results show that the central α-helical region of complexins does not undergo conformational changes upon binding and that it is aligned antiparallel to the four-helix bundle of the SNARE complex. Binding is of high affinity with equilibrium constants of about 10 nM. Furthermore, its on-rate is very rapid, with association rates in the millisecond range, making it an attractive candidate to control a late step in exocytosis following the formation of "*trans*"-SNARE complexes.

Our EPR data, together with our previous NMR experiments (19) suggest that complexins have an unusual fold. The protein is largely α-helical but appears to be devoid of strong tertiary interactions. Isolated helices that do not pack against other structures are rare and so far have not been reported from EPR measurements. Furthermore, binding to the ternary SNARE complex appears not to be associated with major conformational changes, at least not in the region analyzed. The only changes we observed were mobility losses on one side of the presumed helix, suggesting that it packs alongside the SNARE complex. Because only part of the binding domain was analyzed, we do not know whether this applies to the entire interacting surface. Nevertheless, binding of a preformed helical segment to a rigid protein complex does not require conformational adaptations, which may be one of the reasons for the fast binding kinetics. Interestingly, complexin binding was not affected when COOH-terminally truncated variants of synapto-

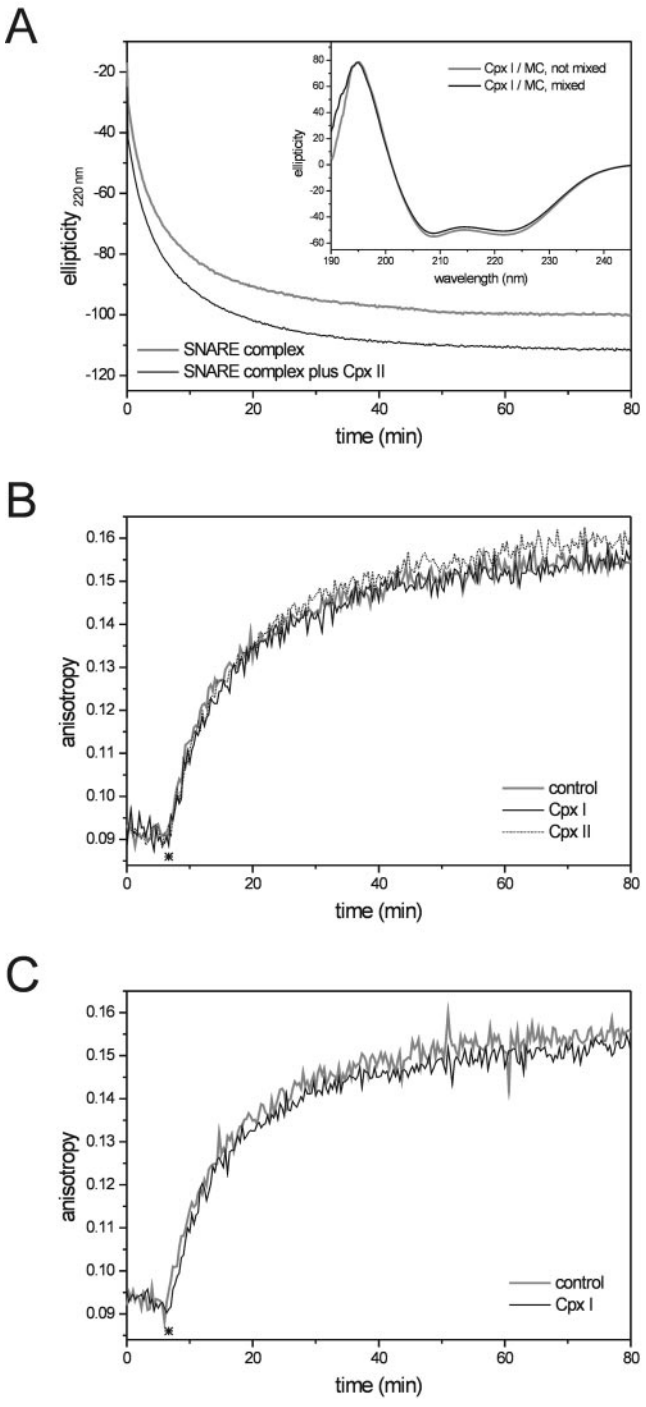

FIG. 7. **Assembly kinetics of the SNARE complex in the presence of complexins.** *Panel A*, addition of complexin I to the assembled minimal core complex (*MC*; see "Experimental Procedures") is not associated with a significant conformational change (*inset*). The CD spectrum recorded for a mix of complexin and minimal core complex (*inset*, *black line*) is similar to the sum of the spectra obtained from the individual components (*inset*, *gray line*). SNARE complex formation was followed by measuring the ellipticity at 220 nm as a function of time (*gray line*). No significant change in the kinetics was observed in the presence of complexin II (*black line*). Note that addition of complexin led to an overall increase in α-helical content because complexin is partially α-helical. *Panels B* and *C*, fluorescence anisotropy of 5 nM SNAP-25, labeled at position 84 with Alexa488 alone (control, *gray lines*) or together with complexin I (*black lines*) or complexin II (*dotted black line*). After 400 s (*asterisks*), a mixture of synaptobrevin and the syntaxin SNARE motif (500 nM each) was added. The increase in anisotropy indicates SNARE complex formation. No changes in the rate of complex formation were observed in the presence of complexin I or II in buffer containing 0.1 mM EDTA (*panel B*) or in the presence of complexin I in 1 mM Ca^{2+} (*panel C*).

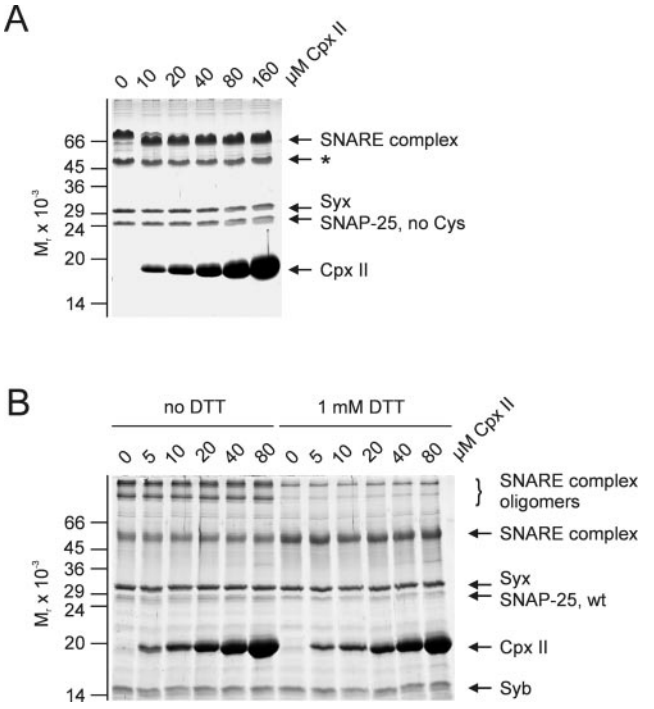

FIG. 8. **Complexin does not induce formation of oligomeric SDS-resistant SNARE complexes.** 10 μM each synaptobrevin (1–96), cysteine-free SNAP-25 (no Cys) in *panel A* or wild type SNAP-25 (*wt*) in *panel B*, and syntaxin 1A (1–262) were incubated with the indicated amounts of complexin II. After at least a 16-h incubation at 4 °C, samples were analyzed without heating by SDS-PAGE and Coomassie Blue staining. No increase in oligomeric SDS-resistant SNARE complexes was observed. Similar results were obtained for complexin I (data not shown). Note that in *panel B* in the absence of DTT more higher molecular weight SDS-resistant bands were visible. These bands were not caused by complexin II because they appeared already in the absence of complexin II. The *asterisk* indicates a shortened SDS-resistant SNARE complex caused by a proteolytic breakdown product of syntaxin. *Syb*, synaptobrevin; *Syx*, syntaxin; *Cpx*, complexin.

brevin or syntaxin were used, suggesting that the region near the membrane anchors of the SNAREs does not participate in complexin binding.

A major conclusion from our data is that complexin only interacts with ternary SNARE complexes and does not influence the rate or the pathway of complex assembly. This issue has previously been controversially discussed. Tokumaru and co-workers (17) have recently proposed that complexin catalyzes the formation of higher order SNARE oligomers, in which the two SNARE motifs of SNAP-25 are part of different complexes, and that complexin dissociates once SNARE complex formation is complete. SNARE oligomers would concentrate assembled SNARE complexes at the site of fusion, greatly accelerating the fusion reaction. Nevertheless, three independent lines of evidence show conclusively that complexin is not involved in SNARE assembly or in the formation of SNARE complex oligomers. First, there is no interaction of complexins with individual SNAREs or with binary syntaxin·SNAP-25 complexes. Although this has been inferred previously from nonequilibrium binding studies (19), we show here that this is also true when all binding partners are present under equilibrium conditions, excluding the possibility that such interaction is of low affinity or that it exhibits a fast off-rate. Second, the rate of SNARE complex formation is not affected, which would be expected if complexin were to direct assembly. Third, we were unable to find any evidence supporting the notion that complexins induce the formation of higher order oligomeric SNARE complexes regardless of whether truncated or full-length SNARE complexes were used, whether equilibrium or

nonequilibrium assays were employed, or whether SNAP-25 was wild type or contained exchanges in the cysteine positions. Only the surface groove lined by syntaxin and synaptobrevin is involved in complexin binding, and it provides a single high affinity binding site. Although attractive, we therefore regard the molecular model proposed by Tokumaru *et al*. (17) as incompatible with the molecular properties of the complexin-SNARE interaction.

How then are the complexins functioning in synaptic vesicle exocytosis, and in which way do they regulate SNARE function? As for many other proteins involved in the control of exocytosis this question cannot be answered conclusively yet. Our data, however, allow us to rule out some models, thus narrowing the number of possibilities. Because we can safely exclude any interaction of complexins with individual SNAREs or binary syntaxin·SNAP-25 complexes, the action of complexin is confined to the steps in the SNARE cycle when SNAREs are assembled. As discussed in the Introduction, SNAREs are thought to assemble into *trans*-complexes before fusion. Influx of calcium probably leads through a yet not understood mechanism to completion of SNARE complex formation and thus to membrane fusion. During fusion, *trans*-SNARE complexes switch into the inactive *cis* configuration, which is then disassembled by the ATPase *N*-ethylmaleimide-sensitive factor in conjunction with cofactors. Complexin knock-out mice show a dramatic reduction in the apparent Ca^{2+} sensitivity of exocytosis (16), suggesting that complexins are involved in linking the Ca^{2+} signal to the exocytotic apparatus. Thus, it is likely that complexins interact with SNARE complexes before membrane fusion. Our analysis indicates that the presence of Ca^{2+} does not substantially alter the complexin-SNARE complex interaction. It is conceivable, however, that complexins modulate the interaction of a Ca^{2+} sensor with the SNARE complex (probably synaptotagmin (35)). Such an explanation is compatible both with the knock-out phenotype and the biochemical and biophysical characteristics of the complexin-SNARE interaction. Moreover, complexin's on-rate in the millisecond time range would allow for its recruitment as soon as the binding site is established during *trans*-SNARE complex formation. Thus, the binding characteristics are in accordance with the control of a transient and short lived intermediate, which may form immediately before exocytosis.

Acknowledgments—We are greatly indebted to Enno Schweineberger for help with the FRET measurements and the calculation of FRET efficiencies and to Rainer Heintzmann for assistance with the stopped-flow data analysis. We also thank Sandra Kriegelstein and Katrin Wiederhold for the generation of cysteine mutants and protein purification and Wolfram Antonin for critically reading the manuscript.

Note Added in Proof—After submission of this paper, the crystal structure of the complexin·SNARE complex was published by another group (Chen, X., Tomchick, D. R., Kovrigin, E., Arac, D., Machius, M., Südhof, T. C., and Rizo, J. (2002) *Neuron* **33,** 397–409).

REFERENCES

1. Neher, E. (1998) *Neuron* **20,** 389–399
2. Jahn, R., and Südhof, T. C. (1999) *Annu. Rev. Biochem.* **68,** 863–911
3. Lin, R. C., and Scheller, R. H. (2000) *Annu. Rev. Cell Dev. Biol.* **16,** 19–49
4. Misura, K. M., May, A. P., and Weis, W. I. (2000) *Curr. Opin. Struct. Biol.* **10,** 662–671
5. Brünger, A. T. (2001) *Curr. Opin. Struct. Biol.* **11,** 163–173
6. Chen, Y. A., and Scheller, R. H. (2001) *Nat. Rev. Mol. Cell. Biol.* **2,** 98–106
7. Rothman, J. E. (1994) *Nature* **372,** 55–63
8. Bock, J. B., Matern, H. T., Peden, A. A., and Scheller, R. H. (2001) *Nature* **409,** 839–841
9. McMahon, H. T., Missler, M., Li, C., and Südhof, T. C. (1995) *Cell* **83,** 111–119
10. Ishizuka, T., Saisu, H., Odani, S., and Abe, T. (1995) *Biochem. Biophys. Res. Commun.* **213,** 1107–1114
11. Takahashi, S., Yamamoto, H., Matsuda, Z., Ogawa, M., Yagyu, K., Taniguchi, T., Miyata, T., Kaba, H., Higuchi, T., Okutani, F., and Fujimoto, S. (1995) *FEBS Lett.* **368,** 455–460
12. Söllner, T., Whiteheart, S. W., Brunner, M., Erdjument-Bromage, H., Geromanos, S., Tempst, P., and Rothman, J. E. (1993) *Nature* **362,** 318–324
13. Sutton, R. B., Fasshauer, D., Jahn, R., and Brünger, A. T. (1998) *Nature* **395,** 347–353
14. Söllner, T., Bennett, M. K., Whiteheart, S. W., Scheller, R. H., and Rothman, J. E. (1993) *Cell* **75,** 409–418
15. Hanson, P. I., Heuser, J. E., and Jahn, R. (1997) *Curr. Opin. Neurobiol.* **7,** 310–315
16. Reim, K., Mansour, M., Varoqueaux, F., McMahon, H. T., Südhof, T. C., Brose, N., and Rosenmund, C. (2001) *Cell* **104,** 71–81
17. Tokumaru, H., Umayahara, K., Pellegrini, L. L., Ishizuka, T., Saisu, H., Betz, H., Augustine, G. J., and Abe, T. (2001) *Cell* **104,** 421–432
18. Ono, S., Baux, G., Sekiguchi, M., Fossier, P., Morel, N. F., Nihonmatsu, I., Hirata, K., Awaji, T., Takahashi, S., and Takahashi, M. (1998) *Eur. J. Neurosci.* **10,** 2143–2152
19. Pabst, S., Hazzard, J. W., Antonin, W., Südhof, T. C., Jahn, R., Rizo, J., and Fasshauer, D. (2000) *J. Biol. Chem.* **275,** 19808–19818
20. Fasshauer, D., Antonin, W., Margittai, M., Pabst, S., and Jahn, R. (1999) *J. Biol. Chem.* **274,** 15440–15446
21. Margittai, M., Fasshauer, D., Pabst, S., Jahn, R., and Langen, R. (2001) *J. Biol. Chem.* **276,** 13169–13177
22. Fasshauer, D., Otto, H., Eliason, W. K., Jahn, R., and Brünger, A. T. (1997) *J. Biol. Chem.* **272,** 28036–28041
23. Fasshauer, D., Bruns, D., Shen, B., Jahn, R., and Brünger, A. T. (1997) *J. Biol. Chem.* **272,** 4582–4590
24. Fasshauer, D., Eliason, W. K., Brünger, A. T., and Jahn, R. (1998) *Biochemistry* **37,** 10354–10362
25. Bradford, M. M. (1976) *Anal. Biochem.* **72,** 248–254
26. Otto, M. R., Lillo, M. P., and Beechem, J. M. (1994) *Biophys. J.* **67,** 2511–2521
27. Laemmli, U. K. (1970) *Nature* **227,** 680–685
28. Hubbell, W. L., McHaourab, H. S., Altenbach, C., and Lietzow, M. A. (1996) *Structure* **4,** 779–783
29. McHaourab, H. S., Lietzow, M. A., Hideg, K., and Hubbell, W. L. (1996) *Biochemistry* **35,** 7692–7704
30. Hubbell, W. L., Gross, A., Langen, R., and Lietzow, M. A. (1998) *Curr. Opin. Struct. Biol.* **8,** 649–656
31. Hubbell, W. L., Cafiso, D. S., and Altenbach, C. (2000) *Nat. Struct. Biol.* **7,** 735–739
32. Xiao, W., Poirier, M. A., Bennett, M. K., and Shin, Y. K. (2001) *Nat. Struct. Biol.* **8,** 308–311
33. Jelesarov, I., and Bosshard, H. R. (1999) *J. Mol. Recognit.* **12,** 3–18
34. Jelesarov, I., and Bosshard, H. R. (1994) *Biochemistry* **33,** 13321–13328
35. Davis, A. F., Bai, J., Fasshauer, D., Wolowick, M. J., Lewis, J. L., and Chapman, E. R. (1999) *Neuron* **24,** 363–376
36. Jares-Erijman, E. A., and Jovin, T. M. (1996) *J. Mol. Biol.* **257,** 597–617

PROTEIN STRUCTURE AND FOLDING:

Rapid and Selective Binding to the Synaptic SNARE Complex Suggests a Modulatory Role of Complexins in Neuroexocytosis

Stefan Pabst, Martin Margittai, Darius Vainius, Ralf Langen, Reinhard Jahn and Dirk Fasshauer

J. Biol. Chem. 2002, 277:7838-7848.
doi: 10.1074/jbc.M109507200 originally published online December 20, 2001